References

[1] B. N. Das, G. S. N. Raju and A. Chakraborty, "Investigations on a new type of inclined slot coupled T-junction," *Proc. Inst. Elec. Eng.*, pt. H, vol. 134, pp. 473–476, 1987.

[2] Powen Hsu and S. H. Chen, "Admittance and resonant length of inclined slots in the narrow wall of a rectangular waveguide," *IEEE Trans. Antennas Propagat.*, vol. 37, pp. 45–49, Jan. 1989.

[3] A. F. Stevenson, "Theory of slots in rectangular waveguides," *J. Appl. Phys.*, vol. 19, pp. 24–38, Jan. 1948.

[4] R. S. Elliott *et al.*, "The scattering characteristics of broad wall slots," Hughes Technical Internal Correspondence, No. 56B1.31/111, Nov. 1, 1983.

[5] B. N. Das, N. V. S. Narasimha Sarma, and A. Chakraborty, "A rigorous variational formulation of an H plane slot coupled tee junction," *IEEE Trans Microwave Theory Tech.*, vol. 38, pp. 93–95, Jan. 1990.

[6] R. F. Harrington, *Time Harmonic Electromagnetic Field*. New York: McGraw-Hill, 1961.

[7] A. A. Oliner, "The impedance properties of narrow radiating slots in the broad face of rectangular waveguide—Parts I and II," *IEEE Trans. Antennas Propagat.*, vol. AP-5, pp. 4–20, Jan. 1957.

Theoretical and Experimental Study of the Evolution of Fields in an Overdimensioned Waveguide with a Corrugated Surface

J. P. Fenelon and A. Papiernik

Abstract—**The field of corrugated waveguides has been extensively investigated over a number of years, as such structures have been used for antenna feeds [1]–[4]. To obtain an answer to problems arising in many microwave applications, some labs use overdimensioned corrugated waveguides. In the present work, we propose a theoretical approach with eigenmodes that enables us to determine the values of the limiting frequencies (frequencies of π modes in the periodic structure) of an overdimensioned parallelepiped cavity loaded with a thin corrugation as a function of the height of the aperture. In this approach, the electric field is represented by different analytical functions. We compared the theoretical results with the experimental values obtained for different apertures and periodicities, according to the value of the wavelength in comparison with the aperture and the period. Each function is in good agreement in a certain frequency range.**

I. Introduction

In a previous study [5], we have shown experimentally that the dispersion characteristic of the periodic structure (period H) in Fig. 1 can be obtained with a cavity loaded by one corrugation (see Fig. 2). The length on either side of the zero-thickness corrugation is $L = kH$ (where k equal $1/2$, 1, $3/2$, $\cdots$ according to the mode studied). The established mode always has the same configuration: the π mode (periodic phase shift $\beta H = \pi$ in the periodic structure).

We used the properties described above (for $L_1 = L_2 = H/2$, the resonant frequency of this cavity corresponding to the limiting frequency of the periodic structure with the same period H) and the "magnetic" eigenvectors to determine the expression for the magnetic field.

Manuscript received January 17, 1989; revised March 6, 1990.

J. P. Fenelon is with I.R.C.O.M., Facultédes Sciences, 123, Avenue Albert Thomas, 87060 Limoges Cedex, France.

A. Papiernik is with the Laboratorire d'Electronique, Université de Nice, Parc Valrose, 06034 Nice Cedex, France.

IEEE Log Number 9101653.

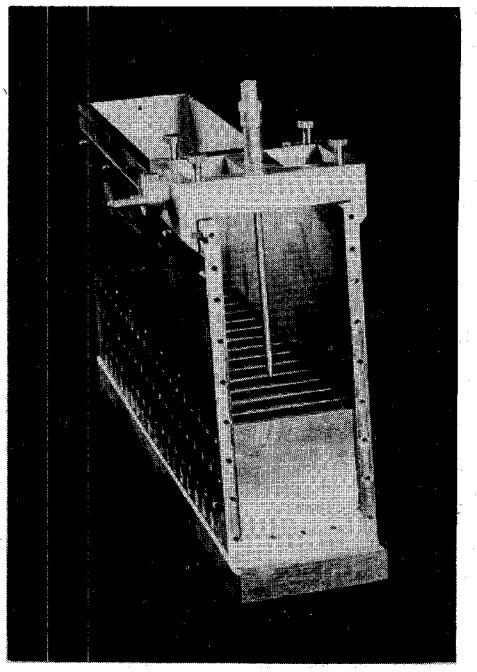

Fig. 1. An overdimensioned rectangular periodic waveguide.

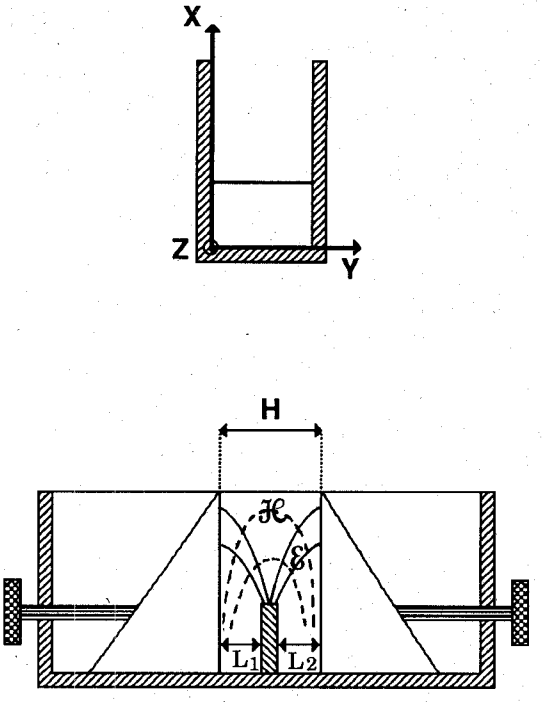

Fig. 2. Equivalent cavity with one corrugation to represent infinite periodic structure. Image of the field configuration in this cavity.

To obtain the theoretical resonant frequency, we assume that in the plane of the zero-thickness corrugation aperture ($x-y$ plane in Fig. 2) the expressions for the electric field components are $E_y = E_z = 0$ and $E_x = f(x)$, where for $f(x)$ we use a distribution, an exponential, and an inverse variation of the square of the distance from the aperture (see Fig. 3) and for the magnetic

0018-9480/91/1000-1773$01.00 ©1991 IEEE

field we write that the $(\vec{H})_y$ component equals zero for $z = 0$ in the aperture.

General Expression for the Magnetic Field

In this subsection, we summarize the paper of Kurokawa [6]. Kurokawa derived the magnetic field in cavities using the following expression:

$$\vec{H} = \sum_a \vec{H}_a \int_v \vec{H} \cdot \vec{H}_a \, dv + \sum_\lambda \vec{G}_\lambda \int_v \vec{H} \cdot \vec{G}_\lambda \, dv \tag{1}$$

where $\vec{H}_a$ represents the solenoidal magnetic eigenfunctions, which are related to the corresponding electric eigenfunctions $(\vec{E}_a)$ by

$$\vec{H}_a = \frac{1}{k_a} \operatorname{curl} \vec{E}_a. \tag{2}$$

The $\vec{G}_\lambda$ function in (1) is given by

$$\vec{G}_\lambda = \frac{1}{k_\lambda} \operatorname{grad} \phi_\lambda \tag{3}$$

and the eigenfunctions ϕ_λ satisfy the Helmholtz equation.

$$\nabla^2 \phi_\lambda + k_\lambda^2 \phi_\lambda = 0 \qquad \text{in } v$$
$$\frac{\partial \phi_\lambda}{\partial n} = 0 \qquad \text{on } S \tag{4}$$

where S is the closed surface of the volume V and n is the outer normal unit vector.

By expressing the fields in terms of eigenfunctions and substituting in Maxwell's equation when there is no current in the cavity walls, Kurokawa obtains the following equations:

$$\{j\omega\mu + k_a^2/(\sigma + j\omega\epsilon)\} s_a = -\int (\vec{n} \times \vec{E}) \cdot \vec{H}_a \, dS \tag{5}$$

where

$$s_a = \int_v \vec{H} \cdot \vec{H}_a \, dv$$

and

$$\int (\vec{n} \times \vec{E}) \cdot \vec{G}_\lambda \, dS = -j\omega\mu \cdot r_\lambda \tag{6}$$

where

$$r_\lambda = \int_v \vec{H} \cdot \vec{G}_\lambda \, dv.$$

Therefore the magnetic field can be written as

$$\vec{H} = \sum_a \vec{H}_a s_a + \sum_\lambda \vec{G}_\lambda r_\lambda \tag{7}$$

which is recognized as (1)

II. Analysis

A. Expressions for the Electric Component Eigenfunctions

As a result of symmetry we consider only half of the cavity. Its dimension is $L = H/2$, where H is the period of the corresponding periodic structure. We attempt to obtain a solution for the electromagnetic field of the TE modes with respect to the y direction in the form of a superposition of TE_{m1p} modes.

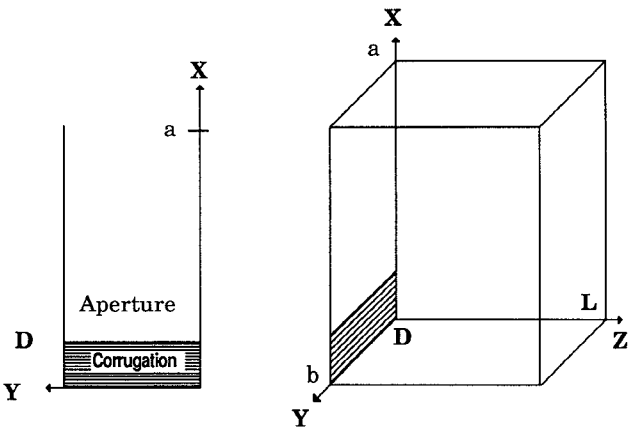

Fig. 3. Views of the cavity studied.

For a rectangular parallelepiped cavity (Fig. 3) the electric component eigenfunctions [7] are given by

$$\vec{E}_a \begin{cases} (e_{m1p})_x = -apbA_{m1p} \cos\dfrac{m\pi}{a}x \sin\dfrac{\pi}{b}y \sin\dfrac{p\pi}{L}z \\ (e_{m1p})_y = 0 \\ (e_{m1p})_z = mLBA_{m1p} \sin\dfrac{m\pi}{a}x \sin\dfrac{\pi}{b}y \cos\dfrac{p\pi}{L}z \end{cases} \tag{8}$$

where A_{m1p} is a normalization factor. To normalize the e_{m1p} we require that

$$\int_v \left[(e_{m1p})_x^2 + (e_{m1p})_y^2 + (e_{m1p})_z^2 \right] dv = 1.$$

Then,

$$A_{m1p}^2 = \frac{2\epsilon_m \epsilon_p \pi^2}{a^3 b^3 L^3} \cdot \frac{1}{k_{m1p}^2 - \left(\dfrac{\pi}{b}\right)^2}$$

where

$$k_{m1p}^2 = \left(\frac{m\pi}{a}\right)^2 + \left(\frac{\pi}{b}\right)^2 + \left(\frac{p\pi}{L}\right)^2$$

for $m = 0, 1, 2, \cdots$; $p = 0, 1, 2, \cdots$; and $m \neq p \neq 0$. Here a, b, and L are the dimensions of the parallelepiped cavity used, and ϵ_m and ϵ_p are Neumann factors.

Now, we can determine the value of the $(\vec{H}_a)_y$ component from (2):

$$\left(\vec{H}_{m1p}\right)_y = \frac{-abL}{\pi} A_{m1p} \frac{k_{m1p}^2 - \left(\dfrac{\pi}{b}\right)^2}{k_{m1p}} \cos\frac{m\pi}{a}x \sin\frac{\pi y}{b} \cos\frac{p\pi}{L}z. \tag{9}$$

B. Expression for the Irrotational Magnetic Component Eigenfunctions

For the cavity considered here (Fig. 3) and with the homogeneous Neumann boundary conditions satisfied we determine (4), the expression for ϕ_λ.

The $\vec{G}_\lambda$ expressions may be derived by using the general equation (3) as follows:

$$\vec{G}_\lambda \begin{cases} G_x = B_{m1p} mbL \sin\dfrac{m\pi}{a}x \cos\dfrac{\pi}{b}y \cos\dfrac{p\pi}{L}z \\ G_y = B_{m1p} aL \cos\dfrac{m\pi}{a}x \sin\dfrac{\pi}{b}y \cos\dfrac{p\pi}{L}z \\ G_z = B_{m1p} pab \cos\dfrac{m\pi}{a}x \cos\dfrac{\pi}{b}y \sin\dfrac{p\pi}{L}z \end{cases} \quad (10)$$

where

$$B_{m1p}^2 = \frac{2\epsilon_m \epsilon_p \pi^2}{a^3 b^3 L^3} \cdot \frac{1}{k_{m1p}^2}.$$

C. Governing Equation for the Electromagnetic Field

We assume that the electric field in the plane of the zero-thickness corrugation aperture at $x = D$ is $E_y = E_z = 0$ and $E_x = f(x)$. In (5), for the electric field expression, we write

$$(\vec{n} \times \vec{E})_y = f(x) \sin\frac{\pi y}{b} \sin\omega t. \quad (11)$$

Using expressions (5), (9), and (11), s_a and r_λ can for $z = 0$ be expressed as

$$s_{m1p} = \frac{\omega}{\omega_{m1p}^2 - \omega^2} \cdot \frac{abL}{\mu\pi} \cdot \frac{b}{2} \cdot A_{m1p} \cdot \frac{k_{m1p}^2 - \left(\frac{\pi}{b}\right)^2}{k_{m1p}} \cdot \cos\omega t \int_D^a f(x) \cdot \cos\frac{m\pi}{a}x\,dx \quad (12)$$

$$r_{m1p} = -\frac{1}{\omega\mu} \cdot \frac{abL}{2} \cdot B_{m1p} \cdot \cos\omega t \int_D^a f(x) \cdot \cos\frac{m\pi}{a}x\,dx. \quad (13)$$

III. Determination of the Resonant Frequency

We note that $(\vec{H})_y = 0$ at $z = 0$, so that we may express the value of $(H)_y$ from (7):

$$(\vec{H})_y = \sum_{mp} \left(\vec{H}_{m1p}\right)_y s_{m1p} + \sum_{mp} \left(\vec{G}_{m1p}\right)_y r_{m1p}. \quad (14)$$

Using (9), (10), (12), and (13), after simplification and substituting A_{m1p}^2 and B_{m1p}^2, a straightforward calculation gives

$$S = (\vec{H})_y = \sum_p \sum_m \frac{(-1)^m \epsilon_m \epsilon_p}{k_{m1p}^2 - \left(\frac{\omega}{c}\right)^2} \int_D^a f(x) \cos\frac{m\pi}{a}x\,dx = 0 \quad (15)$$

with $k_{m1p}^2 = (m\pi/a)^2 + (\pi/b)^2 + (p\pi/L)^2$ and $m \neq p \neq 0$ so, (15) must be decomposed as $S_{mo} + S_{mp} = 0$, where

$$S_{mo} = 2 \sum_{m=1}^{\infty} \frac{(-1)^m}{\left(\frac{m\pi}{a}\right)^2 + \left(\frac{\pi}{b}\right)^2 - \left(\frac{\omega}{c}\right)^2} \cdot \int_D^a f(x) \cos\frac{m\pi}{a}x\,dx \quad (16a)$$

and

$$S_{mp} = 4 \sum_{m=1}^{\infty} \sum_{p=1}^{\infty} \frac{(-1)^m}{\left(\frac{p\pi}{L}\right)^2 + \left(\frac{m\pi}{a}\right)^2 + \left(\frac{\pi}{b}\right)^2 - \left(\frac{\omega}{c}\right)^2} \cdot \int_D^a f(x) \cos\frac{m\pi}{a}x\,dx. \quad (16b)$$

The roots of (16) give the resonant frequencies for a given $f(x)$. For $f(x)$ we use

$$f(x) = \delta(x - D).$$

A field singularity appears in the presence of a corrugation edge, and prompts us to use a field variation in the form of a distribution.

$$f(x) = e^{-k_x x} \quad \text{where} \quad k_x^2 = \left(\frac{\pi}{2L}\right)^2 - \left[\left(\frac{\omega}{c}\right)^2 - \left(\frac{\pi}{b}\right)^2\right].$$

The results found in [8] show that an exponential variation can be a good solution.

$$f(x) = \frac{1}{\sqrt{(a-D)^2 - (a-x)^2}}.$$

On the other hand, the paper by Bethe and Meixner in [9] shows that the field near the corrugation satisfies this function.

A. Distribution Function [10]

Replacing $f(x)$ by $\delta(x - D)$, (16a) gives summations with respect to m which are obtained using the relationships in the Appendix. For all following equations we put

$$W^2 = \left(\frac{\omega}{c}\right)^2 - \left(\frac{\pi}{b}\right)^2$$

$$S_{mo} = \frac{-a\cos DW}{W \sin aW} + \frac{1}{W^2}. \quad (17)$$

Equation (16b) then gives

$$S_{mp} = 4\left(\frac{a}{\pi}\right)^2 \sum_{p=1}^{\infty} \sum_{m=1}^{\infty} \frac{(-1)^m \cos\frac{m\pi}{a}D}{m^2 + A^2}$$

where

$$A^2 = \left(\frac{a}{\pi}\right)^2 \cdot \left[\left(\frac{p\pi}{L}\right)^2 - W^2\right]. \quad (18)$$

The summations with respect to m are obtained using the relationships in the Appendix; for those with respect to p, only one part is calculated with the relations in the Appendix. It is necessary to distinguish two cases according to the positive or negative values of A^2.

The result of a straightforward calculation of (18) gives, by addition with (17), the equations (19) and (20), whose roots are the resonant frequencies of the cavity. For $A^2 > 0$,

$$\frac{\cos DW}{W \sin aW} - \frac{\frac{L}{a}}{W \tan LW} - 2 \sum_{p=1}^{\infty} \frac{\cosh D\frac{\pi A}{a}}{\frac{\pi A}{a} \sinh \pi A} = 0. \quad (19)$$

For $A^2 < 0$,

$$\frac{\cos DW}{W \sin aW} + \frac{\frac{L}{a}}{W \tan LW} - \frac{\frac{2}{a}}{W^2} + 2 \sum_{p=1}^{\infty} \frac{\cos D\left|\frac{\pi A}{a}\right|}{\left|\frac{\pi A}{a}\right| \sin|\pi A|} = 0. \quad (20)$$

B. Exponential Function [10]

In (16), we substitute $e^{-k_x x}$ for $f(x)$, and after integration with respect to x, we obtain

$$S_{mo}=2\sum_{m=1}^{\infty}\frac{\left[k_x e^{-k_x(a-D)}+(-1)^m\frac{m\pi}{a}\sin\frac{m\pi}{a}D-(-1)^m k_x\cos\frac{m\pi}{a}D\right]}{\left\{m^2-\left(\frac{a}{\pi}\right)^2W^2\right\}\cdot\left\{m^2+\left(\frac{a}{\pi}\right)^2k_x^2\right\}} \tag{21}$$

and

$$S_{mp}=4\sum_{p=1}^{\infty}\sum_{m=1}^{\infty}\frac{\left[k_x e^{-k_x(a-D)}+(-1)^m\frac{m\pi}{a}\sin\frac{m\pi}{a}D-(-1)^m k_x\cos\frac{m\pi}{x}D\right]}{\left(m^2+\left(\frac{a}{L}\right)^2Y_A^2\right)\cdot\left(m^2+\left(\frac{a}{\pi}\right)^2k_x^2\right)} \tag{22}$$

with $Y_A^2=p^2-(L/\pi)^2W^2$ and $k_x^2=(\pi/2L)^2-W^2$. According to the positive or negative values of k_x^2 and Y_A^2, we obtain different expressions for S_{mo} and S_{mp}. Here, we will only give the results for $Y_A^2>0$ and $k_x^2>0$. The other values have been used in a computer program. As a first step, we transform the products of the denominator in (21) and (22) into summations; in a second step we use the expressions for Σ_p and Σ_m in the Appendix, and in a third step we substitute the new expressions of (21) and (22) into equation (16). The final formula is

$$\begin{aligned}
&2\Bigg[e^{-k_x(a-D)}\cdot\left(\frac{-1}{W\tan aW}-\frac{1}{k_x\tanh k_x}\right)\\
&+\frac{1}{k_x}\left(\frac{\sinh Dk_x}{\sinh ak_x}-\frac{\sin DW}{\sin aW}\right)\\
&+\frac{\cos DW}{W\sin aW}+\frac{\cosh Dk_x}{k_x\sinh ak_x}+\left(\frac{\pi}{2L}\right)^2\cdot\frac{(e^{-k_x(a-D)}-1)}{ak_x^2W^2}\Bigg]\\
&+\left(\frac{e^{-k_x(a-D)}-1}{a}\right)\cdot\Bigg[\frac{-2}{k_x^2}+\frac{\left(\frac{L}{\pi}\right)^2}{\frac{1}{4}-\left(\frac{L}{\pi}\right)^2W^2}\\
&\cdot\left(2-\frac{1}{2\left(\frac{L}{\pi}\right)^2W^2}+\frac{\pi}{2\frac{L}{\pi}W\tan LW}\right)\Bigg]\\
&+\sum_{p=1}^{\infty}\frac{1}{p^2-\frac{1}{4}}\cdot\Bigg[e^{-k_x(a-D)}\cdot\left(\frac{-1}{\frac{\pi}{L}Y_A\tanh\frac{\pi a}{L}Y_A}+\frac{1}{k_x\tanh ak_x}\right)\\
&-\frac{1}{k_x}\left(\frac{-\sinh\frac{\pi D}{L}Y_A}{\sinh\frac{\pi a}{L}Y_A}+\frac{\sinh Dk_x}{\sinh ak_x}\right)\\
&+\frac{\cosh\frac{\pi D}{L}Y_A}{\frac{\pi}{L}Y_A\sinh\frac{\pi a}{L}Y_A}-\frac{\cosh Dk_x}{k_x\sinh ak_x}\Bigg]=0.
\end{aligned} \tag{23}$$

We determine the resonant frequencies by solving numerically the previous equation. Similar relationships are found with other combinations of k_x^2 and Y_A^2.

C. Function

In order to describe the aperture field near the corrugation, Bethe and Meixner [9] used this function.

$$f(x)=\frac{1}{\sqrt{(a-D)^2-(a-x)^2}}.$$

We substitute the above function $f(x)$ into (16a) and (16b) and after integration with respect to x we obtain [10]

$$\sum_{m=1}^{\infty}\sum_{p=0}^{\infty}\frac{\epsilon_m\epsilon_p}{k_{m1p}^2-\left(\frac{\omega}{c}\right)^2}J_0\left(\frac{m\pi}{a}(a-D)\right)=0. \tag{24}$$

As in the previous sections, we divide this equation into two parts, S_{mo} and S_{mp}. For S_{mp} we accomplish first of all, the summations with respect to p. Therefore it is necessary to distinguish two cases according to the positive or negative value of

$$Y_B^2=m^2-\left(\frac{a}{\pi}\right)^2W^2.$$

For the case where $Y_B^2>0$, applying the expression for Σ_p in the Appendix, we obtain

$$S_{mo}+S_{mp}=2\left(\frac{La}{\pi}\right)^2\sum_{m=1}^{\infty}\frac{J_0\left(\frac{m\pi}{a}(a-D)\right)}{Y_B\tanh\frac{L}{a}\pi Y_B}=0. \tag{25}$$

The previous relationship does not converge quickly, so in order to improve its convergence, we add and subtract the following expression.

$$\frac{J_0\left(\frac{m\pi}{a}(a-D)\right)}{Y_B^2}. \tag{26}$$

After simplification and substituting Y_B^2, $S_{mo}+S_{mp}$ may be

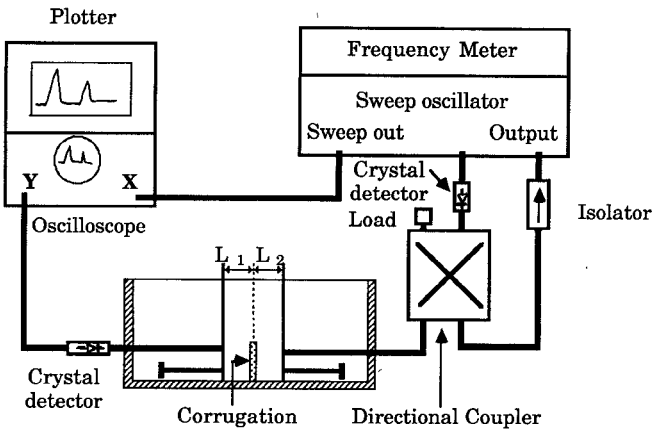

Fig. 4. Experimental mounting to determine the resonant frequencies.

written as follows.

$$\sum_{m=1}^{\infty} \frac{J_0\left(\frac{m\pi}{a}(a-D)\right)}{\sqrt{m^2-\left(\frac{a}{\pi}\right)^2 W^2}} \cdot \left[\frac{2\frac{La}{\pi}}{\tanh\frac{\pi L}{a}\sqrt{m^2-\left(\frac{a}{\pi}\right)^2 W^2}} - \frac{1}{\sqrt{m^2-\left(\frac{a}{\pi}\right)^2 W^2}} \right] + \sum_{m=1}^{\infty} \frac{J_0\left(\frac{m\pi}{a}(a-D)\right)}{m^2-\left(\frac{a}{\pi}\right)^2 W^2} = 0. \quad (27)$$

For the case where $Y_B^2 < 0$, (24) becomes after simplification and using the same manipulation to improve the convergence, we obtain for $S_{mo} + S_{mp}$ the expression

$$\sum_{m=1}^{\infty} \frac{J_0\left(\frac{m\pi}{a}(a-D)\right)}{\sqrt{\left|m^2-\left(\frac{a}{\pi}\right)^2 W^2\right|}} \cdot \left[\frac{-2\frac{La}{\pi}}{\tan\frac{\pi L}{a}\sqrt{\left|m^2-\left(\frac{a}{\pi}\right)^2 W^2\right|}} + \frac{1}{\sqrt{\left|m^2-\left(\frac{a}{\pi}\right)^2 W^2\right|}} \right] + \left(4\left(\frac{a}{\pi}\right)^2 - 1\right) \sum_{m=1}^{\infty} \frac{J_0\left(\frac{m\pi}{a}(a-D)\right)}{\left|m^2-\left(\frac{a}{\pi}\right)^2 W^2\right|} = 0. \quad (28)$$

The resonant frequencies are obtained by numerically computing the roots of (27) and (28).

IV. Results

A. Computed Results

To determine resonant frequencies by a numerical computation we have to solve equations $F(x) = 0$ ((19), (20), (23), (27), and (28)). For that, we fix the values a, b, c and H; for a first value of D from the lower bound $x_0 = 2$ GHz to the upper bound $x_F = 3.5$ GHz, we determine for two values x_A and x_B the sign of $F(x_A) \cdot F(x_B)$.

When $F(x_A) \cdot F(x_B) < 0$, we take the value $x_c = (x_A + x_B)/2$ and we study the sign of $F(x_c) \cdot F(x_A)$ and $F(x_c) \cdot F(x_B)$. We continue the dichotomy and we obtain the first root. According to the values of H and D it is possible to obtain one, two, or three roots between the lower and the upper bound (Figs. 5–8). These roots correspond to the limiting frequencies of the LE_{Y10}, LE_{Y11}, and LE_{Y12} modes of the trough waveguide with periodic corrugation [8] since we have realized our theoretical expressions with the superposition of TE_{m1p} modes.

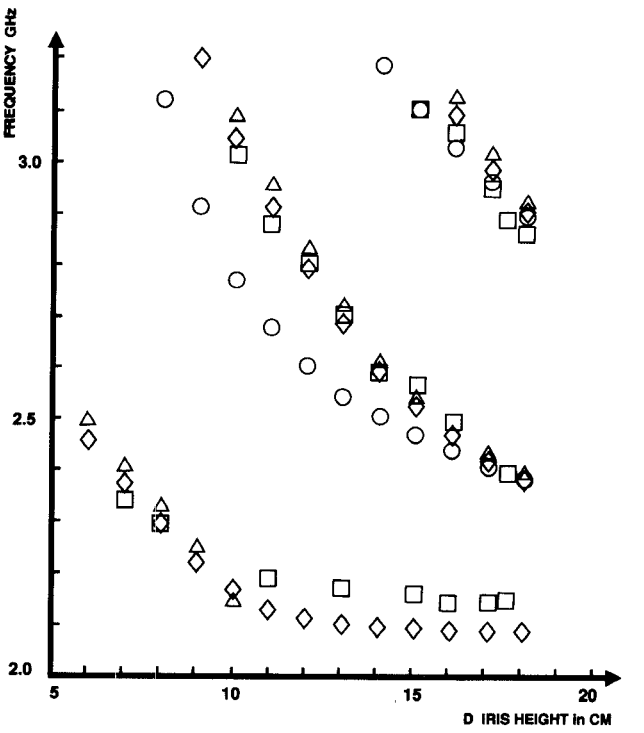

Fig. 5. Theoretical study with three functions: △ distribution, ◇ exponential, and ○ 1/SQRT, □ Experimental study. Period $H = 10$ mm.

B. Experimental Methodology

We use a resonator loaded with one removable corrugation situated between two movable short-circuit plates parallel to the corrugation (Fig. 4). For a fixed value of H ($L_1 = L_2 = H/2$) we determine for each value of D the value of the resonant frequencies of this cavity between 2 and 3.5 GHz given by the sweep oscillator. At the resonance we observe a peak on the oscilloscope and we read this frequency on the frequency meter. It is possible to observe one, two, or three peak. It corresponds to the limiting frequencies of LE_{Y10}, LE_{Y11}, and LE_{Y12} modes of the trough waveguides with the same periodic corrugation (same values for H, for D, and for the thickness: $e = 5$ mm) (Figs. 5–8).

C. Comparison of Theoretical and Experimental Results

We compared the curves found with the theoretical results using the three functions and the experimental values obtained for different apertures and periodicities. We found the following.

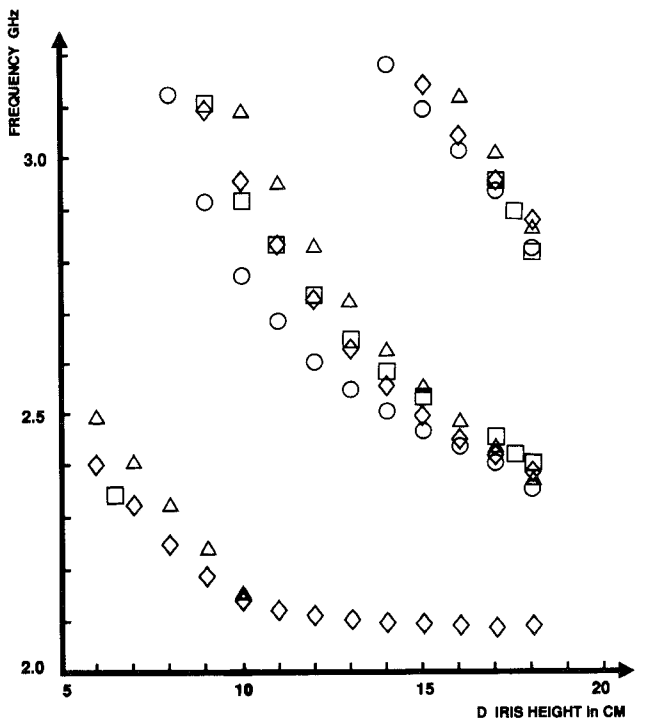

Fig. 6. Theoretical study with three functions: △ distribution, ◇ exponential, and ○ 1/SQRT, □ Experimental study. Period $H = 30$ mm.

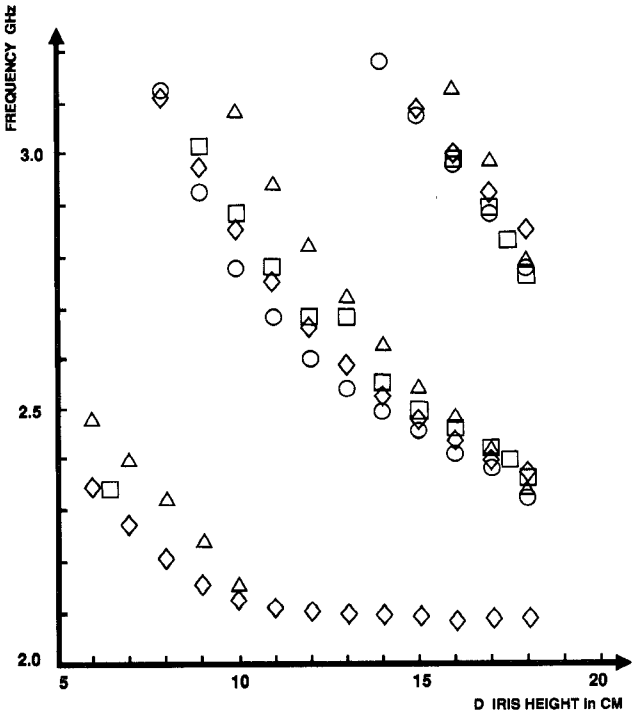

Fig. 7. Theoretical study with three functions: △ distribution, ◇ exponential, and ○ 1/SQRT. □ Experimental study. Period $H = 50$ mm.

1) When we estimate that the field near the corrugation edge is described by a distribution, the experimental and theoretical results agree closely when the values of the period are small compared with the wavelength.

2) When we use Bethe and Meixner's function, we have very good results when the period is in the region of the wavelength and the aperture is small compared with the latter.

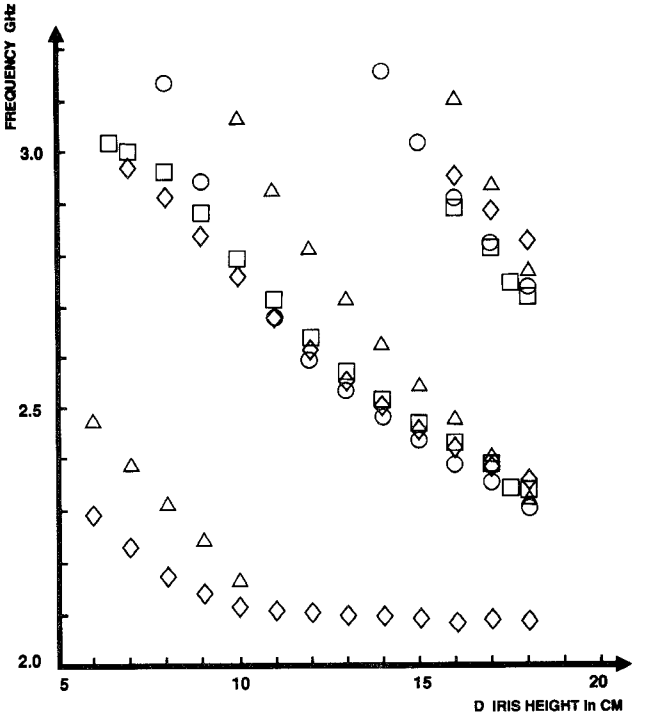

Fig. 8. Theoretical study with three functions: △ distribution, ◇ exponential, and ○ 1/SQRT. □ Experimental study. Period $H = 70$ mm.

3) As a general rule, it is the exponential function which provides, in most cases, results which are in good agreement with experiment. Moreover, it is possible to fully realize the summations with respect to m and so part of those concerning p. So, the results are obtained with a short computing time with a good approximation, the remaining summations having low values compared with the other numerical values.

V. Conclusion

By a theoretical approach with the eigenmodes, we determined the value of the limiting frequency of an overdimensioned rectangular cavity loaded by a zero-thickness corrugation. For that, we assumed that the electric field in the corrugation aperture is a distribution, an exponential variation, and an inverse variation of the square of the distance from the aperture. The theoretical results are obtained when we write that the H_y component of the magnetic field equals zero at the top of the cavity and agrees with experiments. According to the value of the wavelength in comparison with the aperture and the period, each function is in good agreement in certain frequency ranges.

Appendix

With some known expressions [11],

$$\sum_{1}^{\infty} \frac{\cos nx}{n^2+\omega^2} = \frac{\pi}{2}\frac{\cosh \omega(\pi - x)}{\omega \sinh \omega\pi} - \frac{1}{2\omega^2}, \qquad 0 < x < 2\pi$$

$$\sum_{1}^{\infty} \frac{(-1)^n \cos nx}{n^2+\omega^2} = \frac{\pi}{2}\frac{\cosh \omega x}{\omega \sinh \omega\pi} - \frac{1}{2\omega^2}, \qquad -\pi < x < \pi$$

$$\sum_{1}^{\infty} \frac{(-1)^{m-1} m \sin mx}{m^2+B^2} = \frac{\pi}{2}\frac{\sinh xB}{\sinh B\pi}, \qquad -\pi < x < \pi$$

it is possible to deduce for $x = 0$,

$$\sum_1^\infty \frac{1}{n^2+\omega^2} = \frac{\pi}{2\omega \tanh \omega\pi} - \frac{1}{2\omega^2}$$

and for $\omega = ia$, i.e., $\omega^2 = -a^2$,

$$\sum_1^\infty \frac{1}{n^2-a^2} = \frac{-\pi}{2a \tan a\pi} + \frac{1}{2a^2}$$

$$\sum_1^\infty \frac{(-1)^n \cos nx}{n^2-a^2} = \frac{-\pi \cos ax}{2a \sin a\pi} + \frac{1}{2a^2}$$

$$\sum_1^\infty \frac{(-1)^{m-1} m \sin mx}{m^2-A^2} = \frac{\pi}{2} \frac{\sin xA}{\sin \pi A}.$$

References

[1] A. F. Harvey, "Periodic and guiding structures at microwave frequencies," *IRE Trans. Microwave Theory Tech.*, pp. 30–61, Jan. 1960.

[2] G. H. Bryant, "Propagation in corrugated waveguides," *Proc. Inst. Elec. Eng.*, vol. 116, pp. 203–213, Feb. 1969.

[3] Y. Garault, "Hybrid EH guides waves: Their application to microwave separators of High Energy Particules," in *Advances in Microwaves*, vol. 5, L. Young, Ed. New York and London. Academic Press, 1970.

[4] A. J. Sangster and H. G. Donald, "An analysis of an abrupt transition from a uniform empty waveguide to a periodically loaded waveguide," *Int. J. Electron.*, vol. 55, no. 2, pp. 213–227, 1983.

[5] Y. Garault and J. P. Fenelon, "Détermination de la caractéristique de dispersion d'une cavité périodique ouverte à l'aide d'une cavité de longueur variable à un seul iris" ("Determination of the dispersion characteristic of an open periodic structure with the help of a variable length cavity with a single iris") *Comptes-rendus — Académie des Sciences Paris*, vol. 276, série B, pp. 409–412, Mar. 12, 1973.

[6] K. Kurokawa, "The expansions of electromagnetic fields in cavities," *IRE Trans. Microwave Theory Tech.*, vol. 6, pp. 178–187, Apr. 1958.

[7] J. Van Bladel, *Electromagnetic Fields*. New York. McGraw-Hill, 1964.

[8] Y. Garault and J. P. Fenelon, "Les ondes hybrides EH dans un guide en auge périodique." ("Hybrid EH waves in a trough waveguide with periodic corrugation") *Comptes-rendus — Academie des Sciences Paris*, vol. 267, série B, pp. 540–543, Sept. 9, 1968.

[9] R. M. Bevensee, Ed., *Electromagnetic Slow Waves Systems*. New York: Chapter III, pg. 63–91. Wiley, 1964, Ch. III, pp. 63–91.

[10] J. P. Fenelon, Thesis of "Doctorat d'Etat es Sciences" degree, Limoges University, Sept. 5, 1985.

[11] I. S. Gradshteyn and I. M. Ryzhik, *Tables of Integrals, Series and Products*. New York and London: Academic Press, 1965.

Design of New Hybrid-Ring Directional Coupler Using λ/8 or λ/6 Sections

Dong Il Kim and Gyu-Sik Yang

Abstract—**A method for designing 1.25λ-ring and 7λ/6-ring 3 dB directional couplers using fundamental λ/8 or λ/6 sections is proposed and their frequency characteristics are analyzed. Furthermore, experimental verification has been achieved in a microstrip network, confirming the validity of the design method for a microwave component with the basic λ/8 or λ/6 sections proposed in this paper.**

Manuscript received February 22, 1991; revised May 6, 1991. This work was supported by the Korea Science and Engineering Foundation.

The authors are with the Department of Electronics and Communications Engineering, Korea Maritime University, Youngdo-ku, Pusan 606-791, Korea.

IEEE Log Number 9102323.

I. Introduction

The hybrid-ring directional coupler was one of the first and remains one of the most fundamental junctions in the microwave and millimeter-wave frequency bands [1]–[6] where one-axis symmetry is involved. Important properties possessed by all directional couplers are 1) the output arms are isolated from each other and 2) the input arms are matched looking into any arm when the other arms are terminated by matched loads. Since the conventional, simple Y-junction power dividers do not possess these properties, directional couplers are preferable for certain applications, for example antenna array feed systems where the need for minimizing mutual coupling puts a premium on isolation between the output arms of the power dividers [2].

The two-dimensional structure of stripline facilitates construction of the feeding network and antenna elements, such as dipoles, on a single printed circuit board. At high frequencies, some applications make hybrid-ring couplers preferable to branch-line and parallel-line couplers; the former has an inherent 90° phase difference between the output ports. For an antenna array that is fed by an equiphase, symmetrical, corporate network, the hybrid-ring directional coupler has a definite advantage over the parallel-line and branch-line couplers because no phase-compensating element is necessary. The hybrid-ring coupler also has a broader bandwidth than the branch-line coupler [2], [4].

The hybrid-ring directional coupler is well known as a rat race ring which is used for a 3 dB directional coupler with the normalized admittance of $1/\sqrt{2}$ of the entire circumference of the ring [5]. In 1961 Pon proposed a hybrid-ring coupler having a power-split ratio that is proportional to the square of the admittance ratio of the two variable admittances in the ring [2]. In 1982, Kim and Naito developed a broad-band design method of improved hybrid-ring 3 dB directional couplers where the concept of a hypothetical port was adapted [5]. In 1986, Agrawal and Mikucki designed a hybrid-ring directional coupler with arbitrary power divisions by adapting Pon's method to Kim and Naito's concept of a hypothetical port [4]. However, all branch-line couplers, parallel-line couplers, and hybrid-ring couplers, including the rat-race ring, consist of a common fundamental $\lambda/4$ sections. In addition, most microwave components also use fundamental $\lambda/4$ lines.

In this paper, however, we propose a design method for 1.25λ-ring and 7λ/6-ring 3 dB directional couplers using $\lambda/8$ and $\lambda/6$ sections, respectively. In addition, the frequency characteristics of the couplings, together with the isolations, the return losses, and the phase differences between the output ports, are calculated.

II. Analysis and Design of λ/8- and λ/6-Section 3 dB Directional Couplers

The conventional hybrid-ring directional coupler has the configuration shown in Fig. 1 [2]. To increase the degree of freedom of the design, while maintaining symmetry, we can replace the characteristic admittance Y_1 of the $3\lambda/4$ section across the symmetrical axis AA' by Y_3 and replace the lengths $\lambda/4$ and $3\lambda/4$ of two sections across the symmetrical axis AA' by $\lambda/8$